THE JOURNAL OF BIOLOGICAL CHEMISTRY VOL. 286, NO. 32, pp. 28160–28169, August 12, 2011

A Minimal Nuclear Localization Signal (NLS) in Human Phospholipid Scramblase 4 That Binds Only the Minor NLS-binding Site of Importin α1*[S]

Received for publication, February 3, 2011, and in revised form, June 10, 2011 Published, JBC Papers in Press, June 20, 2011, DOI 10.1074/jbc.M111.228007

Kaylen Lott[‡§], Anshul Bhardwaj[‡], Peter J. Sims[¶], and Gino Cingolani[‡1]

From the [‡]Department of Biochemistry and Molecular Biology, Thomas Jefferson University, Philadelphia, Pennsylvania 19107, the [§]Department of Biochemistry and Molecular Biology, SUNY Upstate Medical University, Syracuse, New York 13210, and the [¶]Department of Pathology and Laboratory Medicine, University of Rochester Medical Center, Rochester, New York 14642-8626

Importin α1 can bind *classical* nuclear localization signals (NLSs) in two NLS-binding sites, known as "major" and "minor." The major site is located between ARM repeats 2–4, whereas the minor site spans ARM 7–8. In this study, we have characterized the cellular localization of human phospholipid scramblase 4 (hPLSCR4), a member of the phospholipid scramblase protein family. We identified a minimal NLS in hPLSCR4 (^{273}GSIIRKWN^{280}) that contains only two basic amino acids. This NLS is both necessary for nuclear localization of hPLSCR4 in transfected HeLa cells and sufficient for nuclear import of a non-diffusible cargo in permeabilized cells. Mutation of only one of the two basic residues, Arg^{277}, correlates with loss of nuclear localization, suggesting this amino acid plays a key role in nuclear transport. Crystallographic analysis of mammalian importin α1 in complex with the hPLSCR4-NLS reveals this minimal NLS binds specifically and exclusively to the minor binding site of importin α. These data provide the first structural and functional evidence of a novel NLS-binding mode in importin α1 that uses only the minor groove as the exclusive site for nuclear import of nonclassical cargos.

Phospholipid scramblases (PLSCR)[2] are endofacial plasma membrane proteins, which are conserved from *Caenorhabditis elegans* to humans (1). The human genome encodes four homologous PLSCRs, named hPLSCR1–hPLSCR4 (1). hPLSCR1 is the first identified and better characterized member of this family of proteins. It was originally identified based on its ability to accelerate the transbilayer movement of phospholipids in reconstituted proteoliposomes, in a calcium-dependent manner (2). Despite this demonstrated activity in proteoliposomes, it remains unresolved whether hPLSCR1 and other members of the PLSCR protein family actually contribute to the intracellular calcium-triggered transbilayer movement of phospholipids that is observed in activated platelets and a variety of injured or apoptotic cells (2–6).

In addition to this putative role in phospholipid scrambling, growing evidence suggests an important role of hPLSCR1, and likely other PLSCR family members, as signaling molecules (3, 5). For instance, cytokines such as interferon α can stimulate the transcription of hPLSCR1 (7) and influence its plasma membrane/nuclear distribution (8). Further evidence for a role of PLSCR1 in cell proliferation and differentiation came from PLSCR1-deficient mice, which exhibit impaired proliferation and differentiation of hematopoietic cells in response to stem cell factor and granulocyte colony-stimulating factor (9). The connection between hPLSCR1 and cell proliferation became more apparent from studies showing that hPLSCR1 can translocate into the nucleus in a signal and receptor-dependent manner through the classical nuclear import pathway, which uses importin α/β and Ran (10, 11). In the nucleus, hPLSCR1 has at least two known binding activities. First, it binds the promoter of the inositol 1,4,5-triphosphate (IP_3) receptor type 1 (IP3R1) via an N-terminal DNA-binding motif located between residues 86 and 118 (12). Second, hPLSCR1 interacts with both isoforms of DNA topoisomerase II, and increases the decatenation activity of the isoform IIα (13). The direct role of this nuclear-localized PLSCR1 in mediating the granulocyte colony stimulating factor-induced expansion of granulocyte precursors was recently reported (14). Furthermore, a study of PLSCR3-deficient mice observed a marked reduction in select adipocyte-derived cytokines, impaired glucose tolerance, and marked increase in mass of adipose fat pads (15). This phenotype suggested that the expression of PLSCR3 may be required for normal adipocyte and/or macrophage maturation. Thus, it is becoming apparent that in addition to their putative role in mediating transbilayer lipid movement, PLSCRs have a considerably more complex biology, which is related to and affects cell proliferation and differentiation.

Transport of proteins into the nucleus of eukaryotic cells is an active, signal-mediated process essential for normal cell function (16). Although smaller proteins (molecular mass <40 kDa) can passively diffuse into the nucleus, most proteins are shuttled into the nucleus by dedicated soluble transport factors of the importin β-superfamily (also known as β-karyopherins) (17). Transport receptors specifically recognize nuclear local-

* This work was supported, in whole or in part, by National Institutes of Health Grants 5R01GM074846 (to G. C.) and 5R01HL063819 (to P. J. S.).

[S] The on-line version of this article (available at http://www.jbc.org) contains supplemental Table S1.

The atomic coordinates and structure factors (code 3Q5U) have been deposited in the Protein Data Bank, Research Collaboratory for Structural Bioinformatics, Rutgers University, New Brunswick, NJ (http://www.rcsb.org/).

[1] To whom correspondence should be addressed: 233 South 10th St., Philadelphia, PA 19107. Tel.: 215-503-4573; Fax: 215-923-2117; E-mail: gino.cingolani@jefferson.edu.

[2] The abbreviations used are: PLSCR, phospholipid scramblase; NLS, nuclear localization signal; ARM, armadillo; hPLSCR, human PLSCR; NPC, nuclear pore complex; IBB, importin β-binding; ITC, isothermal titration calorimetry; IP_3, inositol 1,4,5-triphosphate.

ization sequences (NLS) or nuclear export sequences, which act like molecular flags on proteins. In the classical import pathway, a prototypical NLS (18) (exemplified by the SV40 large T-antigen sequence ^{126}PKKKRKV^{132}) is first recognized by the adaptor importin α, which in turn binds importin β through an N-terminal importin β binding (IBB) domain (19). The import complex translocates through the nuclear pore complex (NPC) through binding of the importin β with phenylalanine glycine-containing nucleoporins (FG-nups). Once at the nuclear side of the NPC, the GTPase Ran in its GTP-bound form dissociates importin β from importin α leading to the disassembly of the import complex and release of NLS cargos in the nucleus (16).

Importin β and likely all β-karyopherins are composed of tandem HEAT repeats, which stack on top of one another to form a superhelical solenoid (20, 21). Each HEAT repeat is comprised of two α-helices separated by a turn. Similarly, the adaptor importin α is also built by a repeated helical motif, known as armadillo (ARM), which consists of three α-helices. ARMs stack together to form a helical core (22), which harbors two binding sites for NLSs, a major site, between ARM repeats 2 and 4, and a minor site, between ARM repeats 7 and 8. Classical monopartite NLSs primarily bind the major site, as seen in the SV40 bound structure, although a partially occupied NLS peptide is also seen at the minor binding site (23, 24). By contrast, the bipartite NLS of nucleoplasmin spans the entire NLS-binding groove, occupying both sites (25, 26). In addition to NLSs, the importin α NLS-binding groove can also be occupied by the IBB domain, which functions as an internal autoinhibitory domain (19, 27) and by the N-terminal domain of nucleoporin 50, possibly involved in cargo release (28).

We recently determined the crystal structure of mammalian importin α bound to the hPLSCR1-NLS (11). This work revealed an extended binding interface between importin α and the hPLSCR1-NLS, which binds the major NLS-binding site (ARM 3–4) as well as ARM 1–2, but is not found at the minor NLS-binding site (11). In this paper, we have continued the characterization of human phospholipid scramblases by investigating the cellular expression and nuclear import mechanism of hPLSCR4. Using a combination of cellular, biochemical, and biophysical techniques, we mapped a functional NLS in hPLSCR4 that binds specifically and *exclusively* to the minor NLS-binding site of importin α.

EXPERIMENTAL PROCEDURES

Biochemical Techniques—Human PLSCR4 cDNA was cloned into the pZEOSV2(+/−) plasmid using restriction sites NcoI and HindIII. The palmitoylation-deficient mutant (^{197}AAAFAAPA^{204}) of hPLSCR4 was constructed by oligonucleotide-directed mutagenesis. This construct was used as the template to generate the following alanine mutants in the NLS: the triple mutant R277A/K278A/W279A, the double mutant I275A/I276A, and single mutants R277A, K278A, W279A, and N280A. All plasmids were verified by DNA sequencing. The gene encoding mouse ΔIBB importin α2 (residues 70–529) and full-length human importin α1 (hSRP1α) were purified as previously described (11, 29). Expression and purification of recombinant import factors used for the import assay (RanGDP, RanQ69L, RanBP1, Ntf2, and importin β) were also previously described (30). To generate non-diffusible import cargos, we cloned the DNA region encoding hPLSCR4-NLS (residues 271–283) or hPLSCR1-NLS (residues 255–268) between restriction sites NcoI and BamHI of an engineered pGEX-4T-GFP vector (GE Healthcare) that also encodes the green fluorescent protein (GFP) (30). Both plasmids were expressed in *Escherichia coli* BL21(DE3) cells at 18 °C. The resultant fusion proteins GST-GFP-hPLSCR4-NLS and GST-GFP-hPLSCR1-NLS were purified on glutathione beads followed by gel filtration chromatography on a Superdex S200 column (GE Healthcare).

Cell Culture and Transient Transfection—HeLa S3 cells were cultured in Dulbecco's modified Eagle's medium (Mediatech) supplemented with 10% fetal bovine serum (HyClone). Transient transfection was performed in HeLa cells using Lipofectamine LTX reagent (Invitrogen) following the manufacturer's protocol. After 24–36 h the cells were fixed and GFP fluorescence was visualized using a Leika CTR5000 with a ×40 air objective. The integrity of the GFP-hPLSCR4 fusion protein was determined by Western blot analysis using a rabbit anti-GFP polyclonal antibody (Santa Cruz Biotechnology, Inc.).

Nuclear Import Assay in Permeabilized Cells—Nuclear import assay in digitonin-permeabilized HeLa cells was carried out as previously described (30). HeLa cells were permeabilized with 20 μg/ml of digitonin for 5 min at room temperature in Transport Buffer (TB) (20 mM HEPES, pH 7.3, 110 mM KOAC, 5 mM $Na(OAc)_2$, 2 mM $Mg(OAc)_2$, 2 mM DTT, 1 mM EGTA, 1 μg/ml of leupeptin and pepstatin) (31). All proteins used in the nuclear import assay were in TB. After permeabilization, endogenous importin β-like factors were removed by incubating cells with 5 μM RanQ69L and 150 nM RanBP1 (32). Import reactions were performed in TB using 3 μM importin β, 5 μM Ran, 150 nM NTF2, and 0.7 μM GST-GFP-hPLSCR4-NLS in the presence (or absence) of 3 μM importin α as well as an energy regeneration system (0.1 mM ATP, 0.1 mM GTP, 10 mM creatine phosphate, and 20 units/ml of creatine phosphokinase (33)). Import was allowed to go at 30 °C for 30 min. Cells were immediately fixed, washed with ice-cold PBS, and then visualized using a Leika CTR5000 under a ×40 air objective.

Pulldown Assay and Isothermal Titration Calorimetry (ITC)—For pulldown assay, ΔIBB-importin α1 was covalently cross-linked to cyanogen bromide (CNBr)-activated agarose beads (GE Healthcare). 100 μg of purified GST-GFP-hPLSCR1-NLS, GST-GFP-hPLSCR1-NLS, or a control of free GST-GFP were allowed to incubate with the immobilized importin α for 30 min at room temperature before being washed several times with TB. Bound fractions were eluted with SDS sample buffer and separated on a 12.5% SDS-PAGE. Fractions pulled down by importin α were identified by Western blot analysis using a rabbit anti-GFP polyclonal antibody (Santa Cruz Biotechnology, Inc.). Bands were visualized using a goat anti-rabbit horseradish peroxidase-conjugated secondary antibody (Invitrogen). ITC experiments were carried out at 30 °C in a VP-ITC calorimeter (Microcal), as previously described (34). The hPLSCR4-NLS peptide was dissolved in ITC buffer (10 mM HEPES, pH 7.4, 150 mM sodium chloride, 3 mM EDTA, 1 mM β-mercaptoethanol) at 500 μM final concentration and injected in 10-μl increments into a calorimetric cell containing 1.8 ml of

ΔIBB-importin α (at 65 μM in ITC-buffer). Injections were integrated following manual adjustment of the baselines. ITC data were analyzed using Origin 7.0 data analysis software (Microcal Software, Northampton, MA). Heats of dilution were determined from control experiments with the ITC buffer and subtracted prior to curve fitting using a single set of binding sites model.

Crystallization and Structure Determination—Crystals of mouse ΔIBB-importin α2 in complex with the hPLSCR4-NLS peptide were obtained by adding a 2-fold molar excess of peptide to ΔIBB-importin α2. The complex was equilibrated against ~0.8 M sodium citrate, 100 mM HEPES, pH 6.0, and 10 mM β-mercaptoethanol at 20 °C. 25% glycerol was added to the crystals as cryoprotectant before flash freezing in a nitrogen stream at −170 °C. X-ray data to 2.5-Å resolution were collected on an Oxford Diffraction Xcalibur PX Ultra protein crystallography system equipped with Onyx CCD detector. Data were processed with the Mosflm (35) and further analyzed using CCP4 programs (36). Crystals of the ΔIBB-importin α·hPLSCR4-NLS complex belong to the orthorhombic space group $P2_12_12_1$ (Table 1). The structure was determined by molecular replacement using PHASER (37) and ΔIBB-importin α as search model (PDB code 1Y2A). The initial solution was refined by rigid body refinement, simulated annealing, and isotropic *B*-factor in PHENIX (38). The hPLSCR4-NLS was built in $F_o - F_c$ electron density difference maps using the program Coot (39) followed by positional refinement with PHENIX (38). Water molecules were modeled in 3.5-σ peaks of $F_o - F_c$ density. Further cycles of positional and isotropic *B*-factor refinement with two TLS domains (for ΔIBB-importin α and the hPLSCR4-NLS, respectively) resulted in a final R_{work}/R_{free} ~18.7/22.6% (the R_{free} was calculated using 5% of the observed reflections) (Table 1). The final model includes ΔIBB-importin α2-(75–497), hPLSCR4-NLS-(273–280), and 198 water molecules. 96.6% of residues are in the most favored regions of the Ramachandran plot (Table 1), with only one residue in importin α, Asn^{239}, in a disallowed region. This residue, also an outlier in previous structures of importin α (11), has clear electron density but adopts a non-canonical main chain geometry. Structural figures were made using PyMol (40). Coordinates for the ΔIBB-importin α·hPLSCR4-NLS complex were deposited in the Protein Data Bank with accession code 3Q5U.

RESULTS

Conservation of Functional Motifs in PLSCR4—Isoform 4 of human phospholipid scramblase, hPLSCR4, consists of 329 amino acids and has 46% sequence homology to the better characterized hPLSCR1 (1). hPLSCR4 is predicted to fold into a 12-stranded Tubby-like β-barrel structure that also contains a C-terminal hydrophobic α-helix (Fig. 1), thought to be buried inside the barrel (41). Sequence alignment of human PLSCR isoforms reveals that three motifs important for hPLSCR1 function are also conserved in hPLSCR4 (Fig. 1). First, region 100–132 of hPLSCR4 is ~60% identical to the homologous region of hPLSCR1, which is known to bind to DNA (12). Second, residues 197–204 of hPLSCR4 (^{197}CCCFCCPC^{204}) are highly enriched in cysteines as in hPLSCR1, where this region contains a palmitoylation site (8). Third, like hPLSCR1 (11),

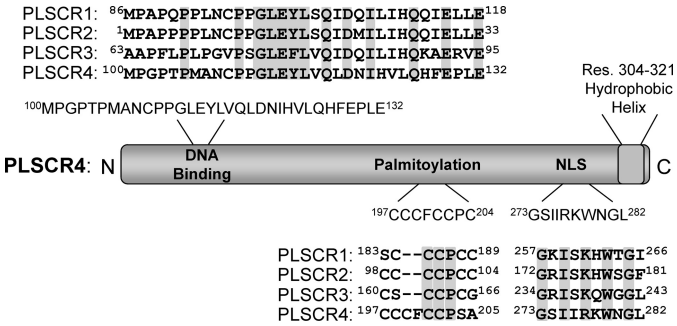

FIGURE 1. **Conservation of functional motifs in hPLSCR4.** Schematic topology of hPLSCR4 showing the amino acid sequence of the putative DNA-binding domain (amino acids 100–132), palmitoylation site (amino acids 197–204), and NLS (amino acids 273–282). For each functional motif in hPLSCR4, a sequence alignment of all PLSCR human isoforms is shown highlighted in *gray* to identical residues conserved in all isoforms.

hPLSCR4 possesses a putative NLS (^{273}GSIIRKWNGL^{282}) that contains only two basic amino acids and is enriched in hydrophobic residues (Fig. 1). However, unlike the hPLSCR1-NLS, this putative NLS lacks a basic residue at the predicted P2 position (Lys^{258} in hPLSCR1-NLS) (11), which in all classical NLSs is essential for binding to importin α and nuclear import (18). Thus, if region 273–282 of hPLSCR4 contains a functional NLS, its binding mode to importin α must be different from that of the many other previously characterized NLSs (18).

Disrupting hPLSCR4 Palmitoylation Site Results in Nuclear Localization—To explore the cellular localization of hPLSCR4, we transiently transfected HeLa cells with a plasmid encoding human hPLSCR4 fused to the green fluorescent protein (GFP-hPLSCR4). GFP was fused to the N terminus of hPLSCR4 to avoid interference with the C-terminal α-helix that is thought to be stabilized inside the β-barrel structure of PLSCRs (41). Attachment of GFP to PLSCR4 results in a fusion protein of ~64 kDa in molecular mass that is above the limit of free diffusion through the NPC. Interestingly, by analogy to hPLSCR1 (11), hPLSCR4 showed a distinct localization at the endofacial surface of the plasma membrane (Fig. 2*A*, *panel 1*). This localization is consistent with palmitoylation of the cysteine-string motif ^{197}CCCFCCPS^{204} (Fig. 1), which possibly anchors hPLSCR4 to the plasma membrane to facilitate lipid binding.

It was previously demonstrated that when the palmitoylation sites are mutated to alanines, hPLSCR1 can enter the cell nucleus through a functional NLS (10, 11). To study the cellular localization of hPLSCR4 when not bound to membranes, we mutated the cysteines critical for palmitoylation to alanines (^{197}AAAFAAPA^{204}). Palmitoylation-mutated hPLSCR4 fused to GFP (GFP-pm-hPLSCR4) was transiently transfected in HeLa cells, where it was expressed with equal efficiency as wild type GFP-hPLSCR4. The localization of hPLSCSR4 was dramatically affected by mutations in the palmitoylation site. When not anchored at the plasma membrane, GFP-pm-hPLSCR4 was able to translocate into the nucleus, where it efficiently accumulated (Fig. 2*A*, *panel 2*). Although some fluorescence signal was still detected in the cytoplasm, the ratio between nuclear/cytoplasmic fluorescence indicates a mainly nuclear localization. Because the GFP-pm-hPLSCR4 fusion protein (molecular mass ~64 kDa) is too large for passive diffusion through the NPC, the nuclear localization of GFP-pm-

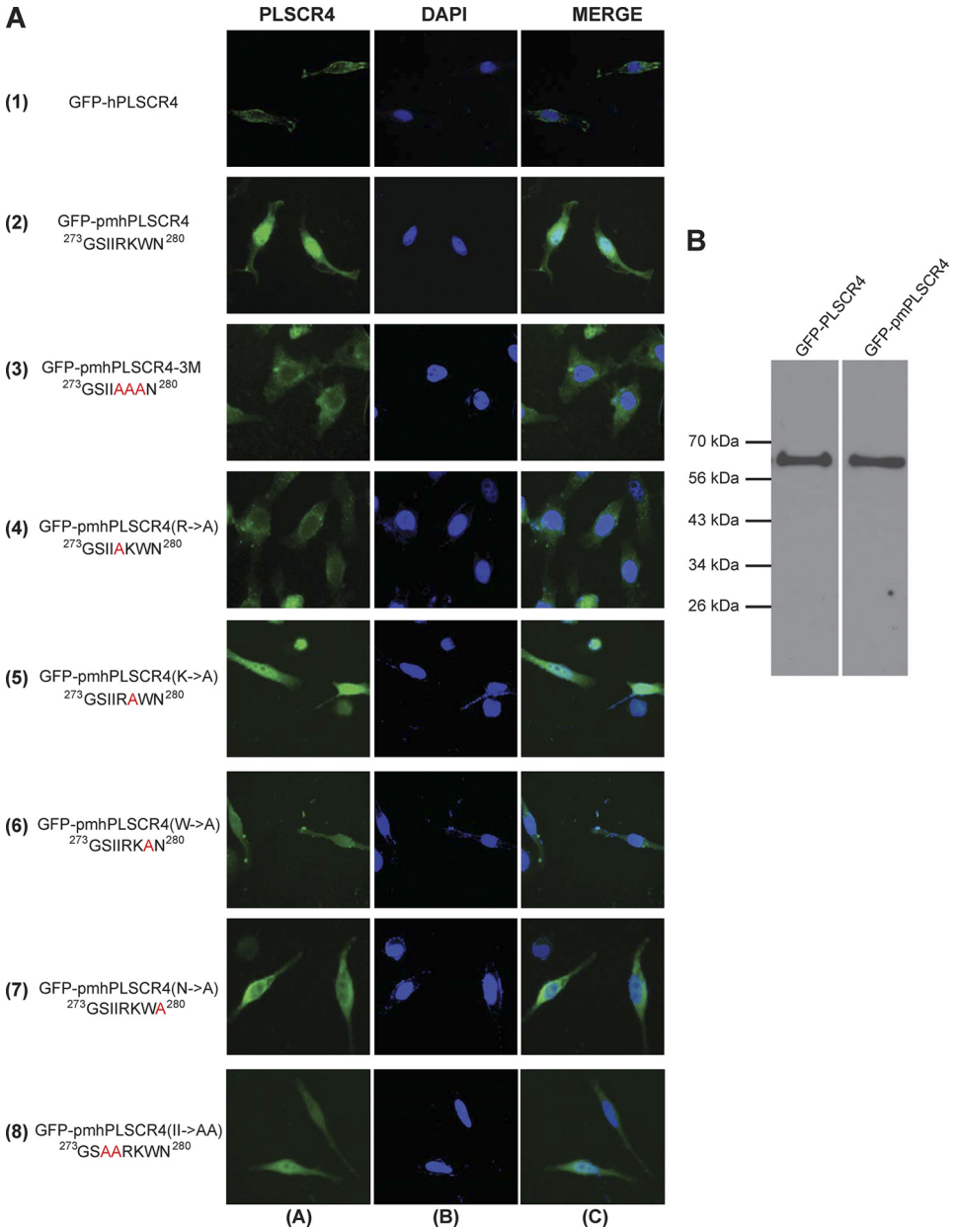

FIGURE 2. **Mutating the palmitoylation site in hPLSCR4 results in efficient nuclear accumulation in HeLa cell.** *A*, representative fluorescent images of HeLa cells transiently transfected with a plasmid encoding different constructs of hPLSCR4 fused to GFP (from top to bottom): *1*, wild-type (WT) hPLSCR4 (GFP-hPLSCR4); *2*, palmitoylation mutant (GFP-pm-hPLSCR4); *3*, NLS triple mutant (GFP-pmhGFP-3M(RKW→AAA)); *4*, single mutants (GFP-pm-hPLSCR4[R→A]); *5*, single mutant (GFP-pm-hPLSCR4[K→A]); *6*, single mutant (GFP-pm-hPLSCR4[W→A]); *7*, single mutant (GFP-pm-hPLSCR4[N→A]); and *8*, the double mutant (GFP-pm-hPLSCR4[II→AA]). Column *A* shows GFP visualization, column *B* are nuclei stained with DAPI, and column *C* is the merged image. *B*, Western blot analysis of HeLa whole cell lysates with an anti-GFP antibody after transient transfection with a plasmid encoding either WT GFP-hPLSCR4 (*lane 1*) or GFP-pm-hPLSCR4 (*lane 2*).

hPLSCR4 is most likely due to active nuclear import. To rule out the possibility that nuclear fluorescence was due to a cleavage product or free GFP (which would be small enough to diffuse into the nucleus), we performed a Western blot analysis of whole cell lysates after transient transfection. Using a monoclonal anti-GFP antibody, we detected only one band corresponding to the expected molecular mass of the GFP-hPLSCR4 fusion protein (molecular mass ~64 kDa) (Fig. 2*B*). This confirmed that the nuclear fluorescence observed in Fig. 2*A*, *panel 2*, corresponds to a protein of mass representing the full-length hPLSCR4 fused to GFP. By analogy to hPLSCR1, nuclear import of GFP-hPLSCR4 is likely mediated by the putative NLS spanning residues 273–282 (Fig. 1).

hPLSCR4 Contains a NLS Necessary for Nuclear Import in HeLa Cells—To study the import mechanism of hPLSCR4, we disrupted the putative NLS by mutating residues ^{277}RKW^{279} to ^{277}AAA^{279}. This construct, GFP-pm-hPLSCR4-3M(^{277}AAA^{279}), was transiently transfected in HeLa cells (Fig. 2*A*, *panel 3*) where it displayed dramatically reduced nuclear localization, as compared with GFP-pm-hPLSCR4. This confirmed that region ^{277}RKW^{279} is part of a functional NLS, which, like in hPLSCR1 (11), is also located at the protein C

terminus (Fig. 1). To further dissect the contribution of individual residues in hPLSCR4-NLS, we introduced individual alanine substitutions at positions Arg^{277}, Lys^{278}, and Trp^{279} (Fig. 2*A*, *panels 4–6*). Strikingly, replacing Arg^{277} resulted in marked reduction in nuclear localization. The construct GFP-pm-hPLSCR4-(Ala^{277}) gave the same pattern of loss of nuclear localization (Fig. 2*A*, *panels 4*) as seen for the triple mutant GFP-pm-hPLSCR4-($^{277}AAA^{279}$) (Fig. 2*A*, *panels 3*). By contrast, none of the single point mutations at Lys^{278}, Trp^{279}, or Asn^{280} abolished nuclear import of hPLSCR4 (Fig. 2*A*, *panels 5–7*, respectively). Likewise, mutating $^{275}II^{276}$ to alanine did not affect nuclear localization of GFP-pm-hPLSCR4-($^{275}AA^{276}$) (Fig. 2*A*, *panel 8*), suggesting these hydrophobic residues are not essential for nuclear import. Thus, hPLSCR4 contains a functional NLS that is necessary to mediate nuclear localization when the protein is not palmitoylated. This NLS contains only two basic residues ($^{277}RK^{278}$), of which only the first, Arg^{277}, is essential for nuclear import in transfected HeLa cells.

hPLSCR4-NLS Is Sufficient for Nuclear Import of a Non-diffusible Cargo in Permeabilized Cells—To determine whether hPLSCR4-NLS contains all determinants sufficient to confer nuclear import, we carried out a nuclear import reaction in digitonin-permeabilized HeLa cells. To prevent passive diffusion into the nucleus, we used a fluorescent chimera of GST-GFP fused to the hPLSCR4-NLS (GST-GFP-hPLSCR4-NLS) as substrate for the import reaction. This cargo (molecular mass ~55 kDa) was excluded from the nucleus of permeabilized HeLa cells when only Transport Buffer (see "Experimental Procedures") was added to permeabilized cells (Fig. 3*A*, *panel A*). By contrast, efficient nuclear import of GST-GFP-hPLSCR4-NLS was observed in the presence of cytosolic HeLa extracts (Fig. 3*A*, *panel B*). Likewise, addition of purified importin α/β, Ran, and Ntf2 also resulted in specific nuclear accumulation of hPLSCR4-NLS (Fig. 3*A*, *panel C*), suggesting an involvement of the classical import pathway. Accordingly, when importin α was removed from the reaction mixture, no significant nuclear accumulation of GST-GFP-hPLSCR4-NLS fusion protein was observed (Fig. 3*A*, *panel D*). Thus, importin α is the functional import adaptor for hPLSCR4-NLS which, like hPLSCR1 (11), enters the cell nucleus through the classical import pathway.

hPLSCR4-NLS Binds Specifically to Importin α—The direct binding of hPLSCR4-NLS to importin α was further characterized using purified recombinant factors. By pulldown assay, the import cargo of GST-GFP-hPLSCR4-NLS was competent for binding to a truncated version of importin α lacking the autoinhibitory IBB domain (ΔIBB-importin α) immobilized on CNBr-agarose beads (Fig. 3*B*). Binding of GST-GFP-hPLSCR4-NLS to ΔIBB-importin α was comparable with that of GST-GFP-hPLSCR1-NLS (Fig. 3*B*, *lanes 5* and *4*, respectively) and specific, as compared with a negative control of free GST-GFP (Fig. 3*B*, *lane 3*). Using ITC, we quantified the dissociation constant (K_d) of hPLSCR4-NLS for ΔIBB-importin α. Titration at 30 °C yielded an exothermic binding reaction that is best described by a single-site hyperbolic binding model (Fig. 3*C*). The curve fitting gave a $K_d = 48.7 \pm 6.5$ μM at 30 °C with an enthalpy of complex formation of $\Delta H = -2{,}961 \pm 119.2$ cal/mol and entropy of binding of $\Delta S = 11.7$ cal/mol. This K_d is very similar to that measured in a control reaction, where the previously characterized hPLSCR1-NLS (11) was titrated into a cell containing ΔIBB-importin α under identical conditions (data not shown). Thus, the hPLSCR4-NLS binds specifically and saturably to importin α with micromolar affinity.

hPLSCR4-NLS Binds Exclusively to the Minor NLS-binding Site of Importin α—To visualize the interaction of importin α1 with hPLSCR4-NLS, we co-crystallized a synthetic peptide comprising this NLS in complex with mouse ΔIBB-importin α2. This murine isoform has 99.2% sequence similarity to the human importin α1 (hSRP1α) used for functional studies in Figs. 2 and 3 but crystallizes more readily than the human isoform. The structure of the ΔIBB-importin α-hPLSCR4-NLS complex was determined to 2.5-Å resolution (Table 1). $F_o - F_c$ electron density difference maps revealed clear electron density for the hPLSCR4-NLS located over the minor NLS binding pocket (Fig. 4*B*), which was not present in the phasing model. Residues ^{273}GSIIRKWN^{280} of hPLSCR4-NLS were modeled in the electron density. The final model (Fig. 4*A*), which includes residues 75–497 of importin α2, 273–281 of hPLSCR4-NLS, and 198 water molecules, was refined to a R_{work}/R_{free} of 18.7 and 22.6%, respectively (Table 1). The refined hPLSCR4-NLS model has an average *B*-factor of 60 Å^2, approximately twice that of importin α. This *B*-factor is in line with that observed for the classical NLSs (23, 24, 26) and the hPLSCR1-NLS (11), which were determined crystallographically to a comparable resolution. Omitting the hPLSCR4-NLS from the structure increases the R_{free} by 1.5%, confirming the peptide is bound to importin α and contributes to the overall structure factors.

The structure revealed that the hPLSCR4-NLS adopts an extended conformation that runs antiparallel to the importin α core (Fig. 4*A*). Notably, this NLS binds only the NLS-minor binding site, between ARM repeats 7 and 8. Unlike the hPLSCR1-NLS (11), and classical NLSs (18), absolutely no electron density for hPLSCR4-NLS was observed at the NLS-major binding site (ARM 2–4), which suggests the minor groove of importin α is the only binding site. Despite the small size (~8 residues), the hPLSCR4-NLS is recognized by importin α with high specificity: at least two structural determinants contribute to this specificity (Fig. 4*C*). First, the hPLSCR4-NLS backbone is contacted and oriented inside the minor NLS-binding pocket by a network of hydrogen bonds with three conserved importin α asparagines, αAsn^{319}, αAsn^{361}, and αAsn^{403}, as well as αAsp^{280}. Similarly, αTrp^{357} packs beneath the hPLSCR4 main chain between residues 280 and 278, further stabilizing the NLS in the minor NLS-binding groove. Second, side chain contacts between hPLSCR4-NLS residues at positions Ser^{274}, Arg^{277}, Lys^{278}, and Asn^{280} and importin α polar residues provide the essential electrostatic binding complementarily to stabilize the NLS in the minor NLS-binding pocket (Fig. 4*C*). Notably, the binding of Arg^{277} to importin α involves a crucial salt bridge between the guanidinium group of hPLSCR4 Arg^{277} and the carboxyl group of αGlu^{396} (Fig. 5*A*). The guanidinium group of Arg^{277} also engages in a close cation-π interaction with the indole ring of αTrp^{399}. The program CaPTURE (cation-π trends ssing realistic electrostatics) (42) predicts the energetic contribution of this interaction to be as high as −5.03 kcal/mol. Accordingly, the ring of αTrp^{399} is only 3.5 Å away from the cationic guanidinium group of Arg^{277} in a parallel geometry

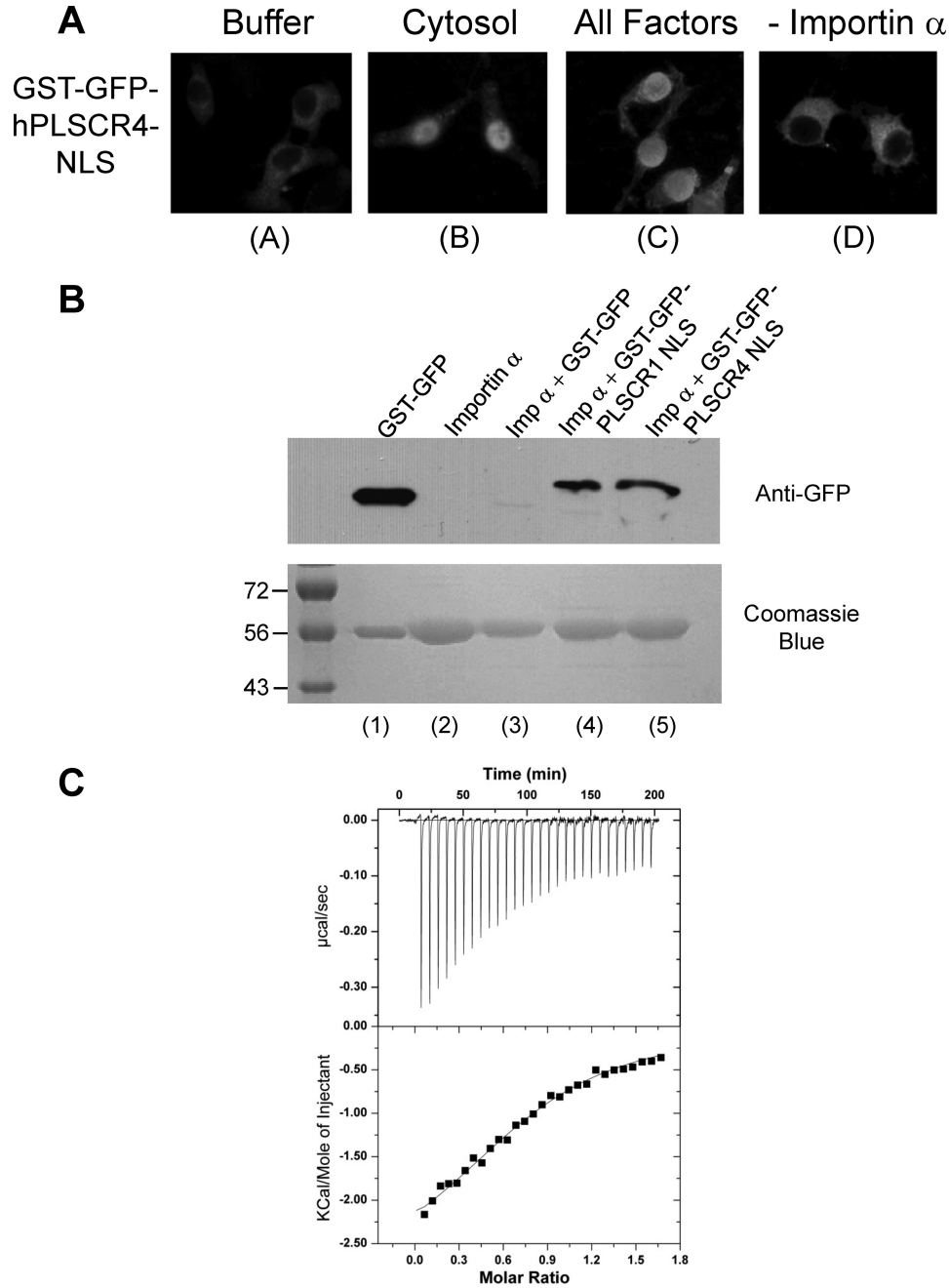

FIGURE 3. **Region 273–282 of hPLSCR4 contains a functional NLS that binds importin α1.** *A*, nuclear import of a non-diffusible GST-GFP-hPLSCR4-NLS chimera in digitonin-permeabilized HeLa cells requires importin α1. From left to right, reactions were carried out in the presence of buffer, cytosolic extracts, all factors (importin β, importin α, NTF2, Ran, plus energy), and all factors except importin α. *B*, pulldown assay. *Top*, a Western blot analysis of fractions probed with an anti-GFP tag antibody. *Bottom*, the SDS gel used for blotting. *Lane 1* is a control of GST-GFP. *Lanes 2* and *3* are controls showing that free ΔIBB-importin α does not interact with the antibody (*lane 2*), and free GST-GFP (*lane 3*) does not interact with ΔIBB-importin α. *Lanes 4* and *5* contain GST-GFP-hPLSCR1-NLS and GST-GFP-hPLSCR4-NLS pulled down by ΔIBB-importin α immobilized on CNBr beads. Notice that GST-GFP-hPLSCR1-NLS and GST-GFP-hPLSCR4-NLS are about 2 kDa larger in molecular mass than free GST-GFP. *C*, ITC analysis of hPLSCR4-NLS binding to ΔIBB-importin α at 30 °C.

(Fig. 5*A*). Finally, the hydrophobic side chain of hPLSCR4-Ile^{275} is positioned less than 4 Å away from the indole group of αTrp^{399} (Fig. 5*A*) further stabilizing the geometry of the cation-π contact this residue makes with hPLSCR4-Arg^{277}. Thus, it appears that much of the interaction between importin α and hPLSCR4-NLS is based on the binding to hPLSCR4-Arg^{277}.

DISCUSSION

hPLSCR4 is one of the four homologues of phospholipid scramblase encoded by the human genome, and possibly the least characterized member of this family (1). In this study, we have characterized the cellular localization of hPLSCR4 in HeLa cells. We provide evidence that hPLSCR4 is sequestered at the plasma membrane by palmitoylation of a Cys-cluster located between residues 197 and 205. In addition, hPLSCR4 can be imported into the nucleus of HeLa cells when its palmitoylation site is mutated. The nuclear import of hPLSCR4 is specifically dependent on a short, poorly basic NLS located at the C terminus of the protein, between residues 273 and 280. This NLS could not be predicted using conventional NLS pre-

TABLE 1
Data collection, phasing, and refinement statistics

Data collection statistics	
Space group	$P2_12_12_1$
Unit cell dimensions (Å)	$a = 77.5, b = 90.9, c = 96.9$
Angles (°)	$\alpha = \beta = \gamma = 90$
Resolution range (Å)	30–2.5
B value from Wilson plot (Å^2)	38.0
Observations (total/unique)	169,480/22,733
Completeness (%)	93.4 (67.3)
R_{sym} [a] (%)	15.9 (68.9)
$\langle I \rangle / \langle \sigma(I) \rangle$	12.9 (2.1)
Refinement statistics	
Number of reflections (30–2.5Å)	22,316
R_{work}/R_{free} [b] (%)	18.7/22.6 (27.2/30.4)
Number of water molecules	198
B value (Å^2): importin α/NLS-peptide/solvent	29.5/60/30
Root mean square deviation from ideal bond length (Å)	0.008
Root mean square deviation from ideal bond angles (°)	1.092
Ramachandran plot (%): core/allowed/generously allowed	96.6/2.9/0.3/0.3

The numbers in parentheses refer to the statistics for the outer resolution shell: (2.62-2.50 Å).
[a] $R_{sym} = \Sigma_{i,h}|I(I,h) - \langle I(h)\rangle|/\Sigma_{i,h}|I(i,h)|$, where $I(i,h)$ and $\langle I(h)\langle$ are the *i*th and mean measurement of intensity of reflection *h*.
[b] The R_{free} value was calculated using 5% of the data.

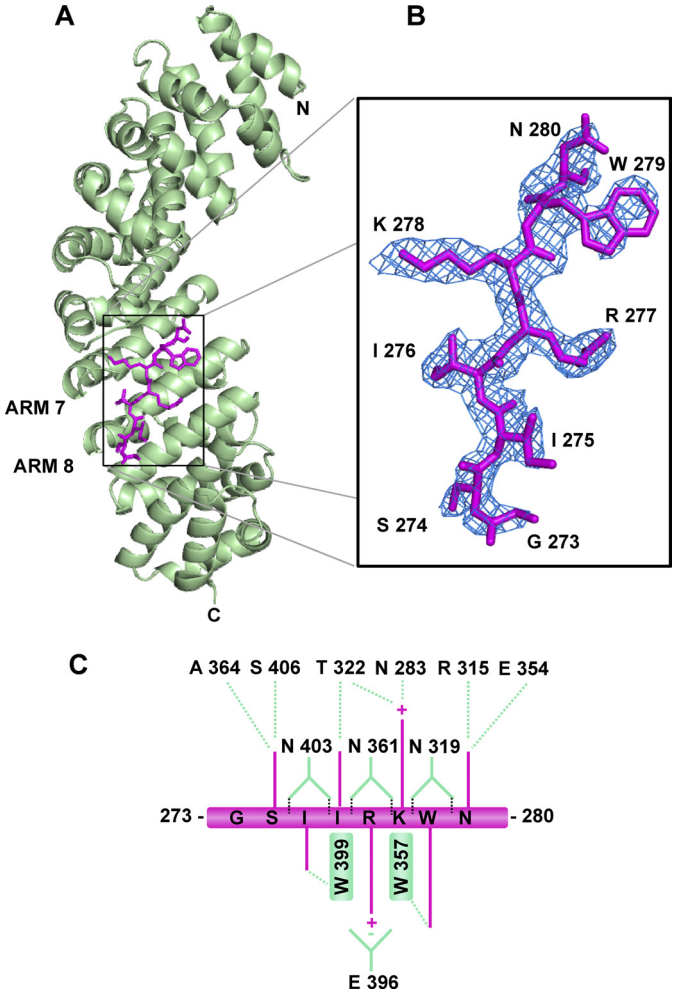

FIGURE 4. **Structure of the ΔIBB-importin α bound to the hPLSCR4-NLS.** *A*, ribbon representation of the mammalian ΔIBB-importin α (in *green*) with the hPLSCR4-NLS (in *magenta*) shown in sticks. The NLS occupies the minor binding groove of importin α (ARM 6–8). *B*, blowup view of the hPLSCR4-NLS refined model superimposed to a final $2F_o - F_c$ electron density map (contoured at 1.25 σ above noise). *C*, schematic diagram of the interaction between ΔIBB-importin α and the hPLSCR4-NLS within a range of 2.5–4.1 Å. In the diagram, the hPLSCR4-NLS is shown in *magenta* and the importin α amino acids in *green*. Key interactions between the hPLSCR4-NLS and importin α at sites P′1—P′5 are also shown under supplemental Table S1.

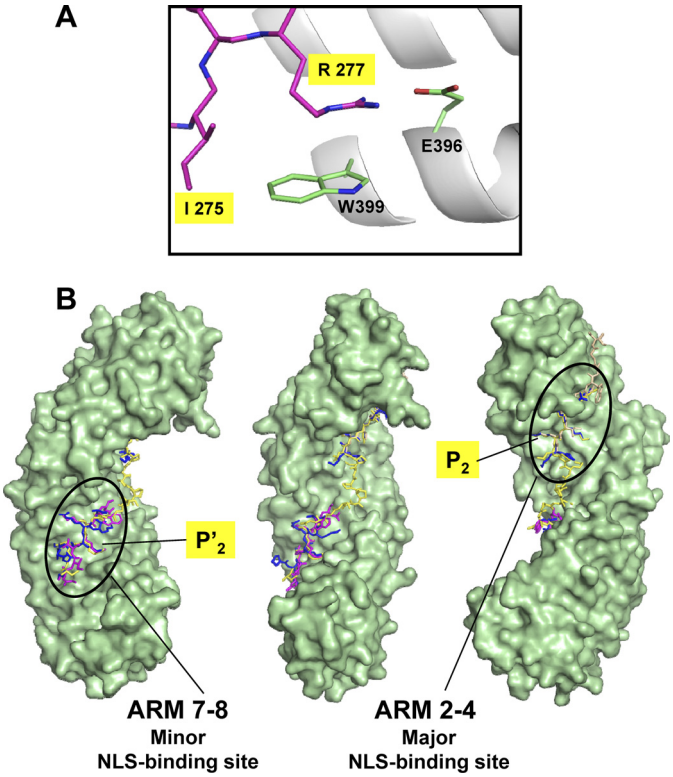

FIGURE 5. **Determinants for recognition of hPLSCR4-NLS by ΔIBB-importin α.** *A*, recognition of hPLSCR4 Arg^{277} by importin α. In the ribbon diagram only two helices of importin α are shown (in *gray*) with two residues, αTrp^{399} and αGlu^{396}, colored in *green*. Arg^{277} and Ile^{275} of the hPLSCR4-NLS are also shown and colored in *magenta*. *B*, structural superimposition of the hPLSCR4-NLS (in *magenta*) with the classical monopartite SV40-NLS (in *blue*), the nucleoplasmin NLS (in *yellow*), and the hPLSCR1-NLS, all mapped onto the structure of ΔIBB-importin α (shown as a *green* surface). The protein is shown in three different views rotated (from left to right) counterclockwise by ~90° with respect to each other. Critical residues at position P_2 and P'_2 of major and minor NLS-binding sites are also shown.

diction algorithms (18) and deviates significantly from the polybasic SV40-like NLS consensus (18). Using a transfection assay in HeLa cells, we demonstrate that the hPLSCR4-NLS is necessary for nuclear localization of hPLSCR4 when the palmitoylation site is removed. Using an *in vitro* nuclear import assay in permeabilized HeLa cells, we show that the hPLSCR4-NLS is

sufficient for nuclear import of a non-diffusible cargo through the classical nuclear pathway that uses importin β/α. *In vitro*, hPLSCR4-NLS binds specifically and saturably to importin α with K_d ~48 μm. Structural characterization of the hPLSCR4-NLS bound to the mammalian importin α reveals this NLS binds specifically and exclusively to the minor NLS-binding site. Although this mode of binding has been hypothesized (43), this is the first structural evidence of an NLS that binds exclusively to the minor groove of importin α.

By analogy to hPLSCR1, the physiological function of hPLSCR4 in the cell nucleus is likely linked to a role in DNA binding that may affect cell proliferation and differentiation. Sequence alignment of human phospholipid scramblases shows that the DNA binding region of hPLSCR1 (residues 86–118), known to interact with the promoter of IP_3 receptor type 1 (IP3R1) (12), is highly conserved in hPLSCR4 (Fig. 1). We propose that the switch controlling nuclear accumulation of hPLSCR4 resides in two functional determinants: the palmitoylation site between residues 197 and 205 and the poorly basic NLS between amino acids 273 and 282 (Fig. 1). The interplay between these two signals is likely to determine the cellular localization of hPLSCR4 and hence its function. Palmitoylation sequesters hPLSCR1 (8) and -4 (and likely other isoforms) at the plasma membrane, facilitating interaction with lipids. However, unlike other post-translational modifications that attach fatty acids to proteins (*e.g.* prenylation, myristoylation, etc.), palmitoylation is fully reversible (44). A class of enzymes known as palmitoyl protein thioesterases break down the ester bond between palmitic acid and protein, freeing up the fatty acid. Loss of palmitoylation in hPLSCR4 correlates with nuclear accumulation, which is mediated by the novel NLS identified and characterized in this paper. Interestingly, several other eukaryotic peripheral membrane proteins, which also function as signaling molecules (*e.g.* Src family kinases, Ras, and the α subunit of heterotrimeric G proteins palmitoylation) are also regulated in a similar manner (44). Therefore, palmitoylation functions by sequestering hPLSCR1 and -4 (and, presumably, the other PLSCR family members) to the plasma membrane unless failure to palmitoylate or, a signal leading to depalmitoylation, permits this normally membrane-tethered protein to traffic to the nucleus as cargo of importin α. Consistent with this idea, it was reported that treating cells with the palmitoylation inhibitor 2-bromo-palmitate results in redistribution of endogenous PLSCR1 from the plasma membrane to nucleus (8). Likewise, nuclear accumulation of hPLSCR1 was also observed by stimulating cultured cells with several cytokines like type I and II interferons (7, 45) and EGF (46). Thus, nuclear localization of hPLSCR4 is highly and specifically regulated in response to extracellular stimuli. The chemistry, specificity, and composition of the hPLSCR4-NLS must reflect this biological plasticity and allow for specific recruitment by importin α only under specific stimulation.

A Minimal NLS That Binds Only the Minor NLS-binding Site of Importin α—Because the discovery of the SV40 large T-antigen NLS (^{126}PKKKRKV^{132}), a cluster of three to five consecutive, positively charged residues has been the crucial characteristic feature of most classical NLSs (supplemental Table S1). In all crystal structures of the yeast and mammalian importin α determined in complex with classical NLS peptides, the minor NLS-binding site of the import adaptor (ARM 7–8) was also found to be partially occupied by an NLS peptide (23–26, 47, 48) (Fig. 5*B*). Except for the bipartite NLS, which spans both NLS-binding sites in importin α (25, 26) (Fig. 5*B*), the physiological significance of having a second monopartite NLS bound at the minor NLS-binding site has remained unclear. Because we have no convincing evidence for importin α binding to two NLS-bearing substrates at the same time, the poorly occupied NLS found at the minor NLS-binding site (23–26, 47, 48) is likely to represent an artifact caused by the large excess of peptide used during crystallization.

In this paper, we demonstrated the hPLSCR4-NLS is both necessary and sufficient for nuclear accumulation of hPLSCR4. Structural analysis reveals that a minimum of two basic residues (Lys^{278} and Arg^{277}) in hPLSCR4-NLS is sufficient to stabilize the peptide in the minor NLS groove of importin α. Arg^{277} (Fig. 5*A*) is responsible for most of the binding energy, due to the multiple interactions with two crucial residues of importin α, Glu^{396} and Trp^{399}. The interaction of Arg^{277} with αTrp^{399} is further stabilized by the hydrophobic contact that another residue in the NLS, hPLSCR4-Ile^{275}, makes with αTrp^{399} (Fig. 5*A*). The structural observation that Arg^{277} is critical for binding of hPLSCR4 to importin α is also corroborated by the fact that Arg^{277} is the only residue in hPLSCR4 that abolishes nuclear localization when mutated to alanine (Fig. 2*A*, *panel 4*). This residue is functionally equivalent to the conserved lysine at position P2 of classical NLS (Lys^{128} in the classical SV40-NLS), which is crucial for nuclear import (supplemental Table S1). Mutation of this residue completely abolishes nuclear import (49), whereas mutation of one of the adjacent basic residues at P1, P3, P4, or P5 reduces, but does not completely abolish nuclear import (50), as seen for mutants at positions P′1, P′3, P′4, and P′5 of the hPLSCR4-NLS (supplemental Table S1).

Kosugi *et al.* (43) recently identified six classes of NLSs that specifically bind importin α. Of these, two classes (class 3 and class 4) were found to specifically bind the minor NLS-binding site of importin α. Interestingly, these two classes of NLSs have two or three basic residues, and have consensus **KR**X(W/F/Y)XXAF and (R/P)XX**KR**(K/R)XX. This minimal NLS is similar to the second basic region of the nucleoplasmin bipartite-NLS (KKKKAQGAKKTAAP**RK**) (25, 26) (Fig. 5*B* and supplemental Table S1). Similarly, other cargos have been reported to bind preferentially or exclusively the minor NLS-binding site. For instance, the autoimmune regulator protein harbors an NLS that binds to the "minor" NLS-binding site of importin α1 and α3 (51). Similarly, Giesecke and Stewart (48) recently reported that the mitotic regulator TPX2 binds to the minor NLS-binding site on importin α via the ^{284}KRKH^{287} region. Thus, the minor NLS-binding site in importin α is a dedicated recognition site that can be occupied by either the smaller basic box of bipartite NLS (but only when simultaneously bound to the major site) or a distinct class of cargos like hPLSCR4.

What is the advantage of binding exclusively to the minor NLS-binding site of importin α? One simple reason has to do with the highly regulated function of proteins like phospholipid

scramblases. It is possible that hPLSCR4-NLS needs to be "minimal" to avoid nuclear translocation under steady state conditions. For instance, members of the phospholipid scramblase family reside primarily at the plasma membrane, where they are tethered to membrane lipids by their multiple thioester-linked palmitates. The presence of a highly basic NLS, such a classical SV40-NLS or a bipartite NLS like in nucleoplasmin would trigger a competition between the soluble nuclear import machinery and the lipid-embedded palmitoyl tail, which could result in extraction of the protein under unstimulated conditions. It is therefore conceivable that a minimal NLS, that makes fewer, yet specific contacts to importin α could be more favorable for a protein that is mainly sequestered at the plasma membrane and would enter the nucleus only under specific conditions (*e.g.* stimulation by interferon (8)). Alternatively, it is possible that certain cargos have developed minimal NLSs that bind only the minor binding site of importin α to avoid competition with most cytosolic classical NLSs, which are constitutively expressed (*e.g.* housekeeping proteins, transcription factors, etc.) and target the major binding site of importin α. The penalty of being a minimal NLS would be to make fewer contacts with importin α, as compared with a classical NLS, which is likely outweighed by binding to a less crowded region of importin α, the minor NLS site. In this respect, the K_d of hPLSCR4-NLS for importin α is only in the low micromolar range. This appears rather weak as compared with nanomolar K_d values usually reported in the literature for classical NLSs (18). However, whereas a micromolar affinity is not likely sufficient to compete for binding to the major NLS site, mainly occupied by nanomolar binders, this affinity is clearly sufficient, both in living (Fig. 2) and permeabilized cells (Fig. 3*A*) to promote importin α-dependent nuclear import of hPLSCR4. The reduced competition for the importin α minor NLS site is the likely cause of this lower binding affinity. Moreover, additional factors may strengthen the affinity of hPLSCR4-NLS for importin α, *in vivo*. For instance, phosphorylation is emerging as an important modification that can enhance the affinity of an NLS cargo for importin α (52). Interestingly, all hPLSCR isoforms have a conserved Ser/Thr within the NLS (Fig. 1) that could potentially be phosphorylated to the increase in binding affinity to importin α. A similar scenario was reported for Epstein-Barr virus nuclear antigen 1 (EBNA-1), whose NLS is also minimal (^{379}KRPRSP*p*SS^{386}), with only two consecutive basic residues. Interestingly, EBNA-1 nuclear translocation is greatly up-regulated by phosphorylation of Ser^{385} within the NLS (53). Although the EBNA-1 NLS is also a micromolar binder *in vitro* ($K_d \sim 60\ \mu$M), phosphorylation of Ser^{385} increases binding affinity for importin α5 by ~20-fold ($K_d \sim 3\ \mu$M) (34), which results in faster nuclear import (53). Further studies will have to clarify if Ser/Thr residues in hPLSCRs-NLS are indeed phosphorylated to promote nuclear accumulation. In conclusion, the work presented in this paper expands the repertoire of NLS that can be recognized by importin α1 and provide a new structural framework to understand the function of the importin α minor-NLS-binding site. The ARM scaffold used by import adaptors provides structural rigidity to expose an extended and versatile binding surface evolved to efficiently accommodate a variety of diverse NLS sequences (Fig. 5*B*). A lower content in basic residues appears to be the fundamental structural determinant that allows a minimal NLS to interact specifically with the minor NLS-binding site, avoiding the competition with more basic NLSs that target the major NLS-binding site of importin α.

Acknowledgments—We thank Honglei Zhou and Dr. Franco Capozza at Thomas Jefferson University for technical help and for the gift of anti-GFP antibody, respectively. ITC and X-ray data were collected at the Kimmel Cancer Center X-ray Crystallography and Molecular Characterization shared resource facility, at Thomas Jefferson University.

REFERENCES

1. Wiedmer, T., Zhou, Q., Kwoh, D. Y., and Sims, P. J. (2000) *Biochim. Biophys. Acta* **1467,** 244–253
2. Zhao, J., Zhou, Q., Wiedmer, T., and Sims, P. J. (1998) *J. Biol. Chem.* **273,** 6603–6606
3. Bevers, E. M., and Williamson, P. L. (2010) *FEBS Lett.* **584,** 2724–2730
4. Zhao, J., Zhou, Q., Wiedmer, T., and Sims, P. J. (1998) *Biochemistry* **37,** 6361–6366
5. Sahu, S. K., Gummadi, S. N., Manoj, N., and Aradhyam, G. K. (2007) *Arch. Biochem. Biophys* **462,** 103–114
6. Suzuki, J., Umeda, M., Sims, P. J., and Nagata, S. (2010) *Nature* **468,** 834–838
7. Zhou, Q., Zhao, J., Al-Zoghaibi, F., Zhou, A., Wiedmer, T., Silverman, R. H., and Sims, P. J. (2000) *Blood* **95,** 2593–2599
8. Wiedmer, T., Zhao, J., Nanjundan, M., and Sims, P. J. (2003) *Biochemistry* **42,** 1227–1233
9. Zhou, Q., Zhao, J., Wiedmer, T., and Sims, P. J. (2002) *Blood* **99,** 4030–4038
10. Ben-Efraim, I., Zhou, Q., Wiedmer, T., Gerace, L., and Sims, P. J. (2004) *Biochemistry* **43,** 3518–3526
11. Chen, M. H., Ben-Efraim, I., Mitrousis, G., Walker-Kopp, N., Sims, P. J., and Cingolani, G. (2005) *J. Biol. Chem.* **280,** 10599–10606
12. Green, D. R., and Evan, G. I. (2002) *Cancer Cell* **1,** 19–30
13. Wyles, J. P., Wu, Z., Mirski, S. E., and Cole, S. P. (2007) *Nucleic Acids Res.* **35,** 4076–4085
14. Chen, C. W., Sowden, M., Zhao, Q., Wiedmer, T., and Sims, P. J. (2011) *J. Leukocyte Biol.* doi:10.1189/jlb.0111006
15. Wiedmer, T., Zhao, J., Li, L., Zhou, Q., Hevener, A., Olefsky, J. M., Curtiss, L. K., and Sims, P. J. (2004) *Proc. Natl. Acad. Sci. U.S.A.* **101,** 13296–13301
16. Stewart, M. (2007) *Nat. Rev. Mol. Cell Biol.* **8,** 195–208
17. Mosammaparast, N., and Pemberton, L. F. (2004) *Trends Cell Biol.* **14,** 547–556
18. Marfori, M., Mynott, A., Ellis, J. J., Mehdi, A. M., Saunders, N. F., Curmi, P. M., Forwood, J. K., Boden, M., and Kobe, B. (2010) *Biochim. Biophys. Acta* doi:10.1016/j.bbamcr.2010.10.013
19. Lott, K., and Cingolani, G. (2010) *Biochim. Biophys. Acta* doi: 10.1016/j.bbamcr.2010.10.012
20. Cook, A., Bono, F., Jinek, M., and Conti, E. (2007) *Annu. Rev. Biochem.* **76,** 647–671
21. Chook, Y. M., and Suel, K. E. (2010) *Biochim. Biophys. Acta* doi: 10.1016/j.bbamcr.2010.10.014
22. Goldfarb, D. S., Corbett, A. H., Mason, D. A., Harreman, M. T., and Adam, S. A. (2004) *Trends Cell Biol.* **14,** 505–514
23. Conti, E., Uy, M., Leighton, L., Blobel, G., and Kuriyan, J. (1998) *Cell* **94,** 193–204
24. Fontes, M. R., Teh, T., and Kobe, B. (2000) *J. Mol. Biol.* **297,** 1183–1194
25. Fontes, M. R., Teh, T., Jans, D., Brinkworth, R. I., and Kobe, B. (2003) *J. Biol. Chem.* **278,** 27981–27987
26. Conti, E., and Kuriyan, J. (2000) *Structure Fold Des.* **8,** 329–338
27. Kobe, B. (1999) *Nat. Struct. Biol.* **6,** 388–397
28. Matsuura, Y., and Stewart, M. (2005) *EMBO J.* **24,** 3681–3689
29. Weis, K., Mattaj, I. W., and Lamond, A. I. (1995) *Science* **268,** 1049–1053
30. Lott, K., Bhardwaj, A., Mitrousis, G., Pante, N., and Cingolani, G. (2010)

J. Biol. Chem. **285,** 13769–13780
31. Adam, S. A., Marr, R. S., and Gerace, L. (1990) *J. Cell Biol.* **111,** 807–816
32. Kutay, U., Izaurralde, E., Bischoff, F. R., Mattaj, I. W., and Görlich, D. (1997) *EMBO J.* **16,** 1153–1163
33. Weis, K., Dingwall, C., and Lamond, A. I. (1996) *EMBO J.* **15,** 7120–7128
34. Nardozzi, J., Wenta, N., Yasuhara, N., Vinkemeier, U., and Cingolani, G. (2010) *J. Mol. Biol.* **402,** 83–100
35. Leslie, A. G. W. (1992) *Joint CCP4 + ESF-EAMCB Newsletter on Protein Crystallography No.* 26 *Protein Crystallography*, CCLRC Daresbury Laboratory, Warrington, UK
36. Collaborative Computational Project Number 4 (1994) *Acta Crystallogr. D Biol. Crystallogr.* **50,** 760–763
37. McCoy, A. J., Grosse-Kunstleve, R. W., Adams, P. D., Winn, M. D., Storoni, L. C., and Read, R. J. (2007) *J. Appl. Crystallogr.* **40,** 658–674
38. Adams, P. D., Afonine, P. V., Bunkóczi, G., Chen, V. B., Davis, I. W., Echols, N., Headd, J. J., Hung, L. W., Kapral, G. J., Grosse-Kunstleve, R. W., McCoy, A. J., Moriarty, N. W., Oeffner, R., Read, R. J., Richardson, D. C., Richardson, J. S., Terwilliger, T. C., and Zwart, P. H. (2010) *Acta Crystallogr. D Biol. Crystallogr.* **66,** 213–221
39. Emsley, P., and Cowtan, K. (2004) *Acta Crystallogr. D Biol. Crystallogr.* **60,** 2126–2132
40. DeLano, W. L. (2002) *The PyMOL Molecular Graphics System*, Schrödinger, LLC, New York
41. Bateman, A., Finn, R. D., Sims, P. J., Wiedmer, T., Biegert, A., and Söding, J. (2009) *Bioinformatics* **25,** 159–162
42. Gallivan, J. P., and Dougherty, D. A. (1999) *Proc. Natl. Acad. Sci. U.S.A.* **96,** 9459–9464
43. Kosugi, S., Hasebe, M., Matsumura, N., Takashima, H., Miyamoto-Sato, E., Tomita, M., and Yanagawa, H. (2009) *J. Biol. Chem.* **284,** 478–485
44. Bijlmakers, M. J., and Marsh, M. (2003) *Trends Cell Biol.* **13,** 32–42
45. Der, S. D., Zhou, A., Williams, B. R., and Silverman, R. H. (1998) *Proc. Natl. Acad. Sci. U.S.A.* **95,** 15623–15628
46. Sun, J., Nanjundan, M., Pike, L. J., Wiedmer, T., and Sims, P. J. (2002) *Biochemistry* **41,** 6338–6345
47. Fontes, M. R., Teh, T., Toth, G., John, A., Pavo, I., Jans, D. A., and Kobe, B. (2003) *Biochem. J.* **375,** 339–349
48. Giesecke, A., and Stewart, M. (2010) *J. Biol. Chem.* **285,** 17628–17635
49. Kalderon, D., Roberts, B. L., Richardson, W. D., and Smith, A. E. (1984) *Cell* **39,** 499–509
50. Colledge, W. H., Richardson, W. D., Edge, M. D., and Smith, A. E. (1986) *Mol. Cell. Biol.* **6,** 4136–4139
51. Ilmarinen, T., Melén, K., Kangas, H., Julkunen, I., Ulmanen, I., and Eskelin, P. (2006) *FEBS J.* **273,** 315–324
52. Nardozzi, J. D., Lott, K., and Cingolani, G. (2010) *Cell Commun. Signal.* **8,** 32
53. Kitamura, R., Sekimoto, T., Ito, S., Harada, S., Yamagata, H., Masai, H., Yoneda, Y., and Yanagi, K. (2006) *J. Virol.* **80,** 1979–1991